



This discussion paper is/has been under review for the journal Atmospheric Chemistry and Physics (ACP). Please refer to the corresponding final paper in ACP if available.

Ice nucleation by combustion ash particles at conditions relevant to mixed-phase clouds

N. S. Umo¹, B. J. Murray¹, M. T. Baeza-Romero², J. M. Jones³,
A. R. Lea-Langton³, T. L. Malkin¹, D. O’Sullivan¹, J. M. C. Plane⁴, and
A. Williams³

¹Institute for Climate and Atmospheric Science, School of Earth and Environment, University of Leeds, Leeds, LS2 9JT, UK

²Escuela de Ingeniería Industrial de Toledo, Universidad de Castilla la Mancha, Avenida Carlos III s/n, Real Fábrica de Armas, 45071 Toledo, Spain

³Energy Research Institute/CFD Centre, Faculty of Engineering, University of Leeds, Leeds, LS2 9JT, UK

⁴School of Chemistry, University of Leeds, Leeds, LS2 9JT, UK

Received: 28 October 2014 – Accepted: 29 October 2014 – Published: 19 November 2014

Correspondence to: N. S. Umo (eensu@leeds.ac.uk) and
B. J. Murray (b.j.murray@leeds.ac.uk)

Published by Copernicus Publications on behalf of the European Geosciences Union.

Ice nucleation by
combustion ash
particles at
conditions relevant to
mixed-phase clouds

N. S. Umo et al.

Title Page

Abstract

Introduction

Conclusions

References

Tables

Figures

◀

▶

◀

▶

Back

Close

Full Screen / Esc

Printer-friendly Version

Interactive Discussion



Abstract

Ice nucleating particles can modify cloud properties with implications for climate and the hydrological cycle; hence, it is important to understand which aerosol particle types nucleate ice and how efficiently they do so. It has been shown that aerosol particles such as natural dusts, volcanic ash, bacteria and pollen can act as ice nucleating particles, but the ice nucleating ability of combustion ashes has not been studied. Combustion ashes are major by-products released during the combustion of solid fuels and a significant amount of these ashes are emitted into the atmosphere either during combustion or via aerosolization of bottom ashes. Here, we show that combustion ashes (coal fly ash, wood bottom ash, domestic bottom ash, and coal bottom ash) nucleate ice in the immersion mode at conditions relevant to mixed-phase clouds. Hence, combustion ashes could play an important role in primary ice formation in mixed-phase clouds, especially in clouds that are formed near the emission source of these aerosol particles. In order to quantitatively assess the impact of combustion ashes on mixed-phase clouds, we propose that the atmospheric abundance of combustion ashes should be quantified since up to now they have mostly been classified together with mineral dust particles. Also, in reporting ice residue compositions, a distinction should be made between natural mineral dusts and combustion ashes in order to quantify the contribution of combustion ashes to atmospheric ice nucleation.

1 Introduction

Combustion processes – either natural or anthropogenic – are a major source of atmospheric aerosol particles (Bond et al., 2013; Li et al., 2003; Pósfai et al., 2003). Various combustion by-products are released directly or indirectly into the atmosphere. These include black and brown carbon, soot, ashes, tar balls, volatile organic compounds (VOCs), and other gases (Petters et al., 2009; Posfai et al., 2004; Fitzpatrick et al., 2008; Williams et al., 2012). These by-products can impact on air quality, health

Ice nucleation by combustion ash particles at conditions relevant to mixed-phase clouds

N. S. Umo et al.

Title Page

Abstract

Introduction

Conclusions

References

Tables

Figures

◀

▶

◀

▶

Back

Close

Full Screen / Esc

Printer-friendly Version

Interactive Discussion



Ice nucleation by combustion ash particles at conditions relevant to mixed-phase clouds

N. S. Umo et al.

Title Page

Abstract

Introduction

Conclusions

References

Tables

Figures

◀

▶

◀

▶

Back

Close

Full Screen / Esc

Printer-friendly Version

Interactive Discussion

and visibility. Additionally, they can influence cloud properties and hence, the Earth's climate (Forster, 2007; Jacobson, 2014). These combustion particles can impact cloud properties by acting as cloud condensation nuclei (CCN) (Spracklen et al., 2011) and potentially as ice nucleating particles (INPs) (Murray et al., 2012; Hoose and Möhler, 2012; Petters et al., 2009).

Ice nucleation can occur via various pathways: deposition nucleation entails ice formation below water saturation where bulk liquid water cannot exist; contact freezing occurs when a particle comes in contact with an interface of a supercooled water droplet; immersion ice nucleation happens when a particle is fully immersed in a water droplet; condensation freezing is rather more poorly defined, but involves the formation of ice as a CCN activates (Vali, 1985; Vali et al., 2014). Of these ice nucleation pathways, immersion mode is argued to be the dominant process for primary ice nucleation in mixed-phase clouds (0––36 °C) (Bond et al., 2013; Murray et al., 2012; Ansmann et al., 2009); hence, we focus here on mixed-phase cloud conditions.

The ice nucleation abilities of some soot types (DeMott, 1990; Kireeva et al., 2009; Popovicheva et al., 2008) and emissions from controlled burns of a range of plant fuels (Petters et al., 2009) in the immersion/condensation mode have been reported, but there is no data on the ice nucleation activities of combustion ashes. Field studies have reported the presence of combustion ashes in atmospheric aerosols (Li and Shao, 2009; Li et al., 2011) and ice crystal residues (DeMott et al., 2003; Kumai, 1961; Cziczo et al., 2004) based on a combination of elemental composition and morphology. However, the distinction between mineral dust and combustion ash is often not done because they have similar compositions.

There are similarities between the elemental composition of fly ash and mineral dust (Chen et al., 2012), which means that it is a challenge to distinguish them using mass spectrometry and other techniques. Consequently, many ice crystal residue studies attributed all mineral compositions to natural dusts although in part it could be due to fly ashes. It is therefore important for the contribution of combustion ashes to atmospheric INPs to be considered. Moreover, given that some mineral dusts are relatively

good INPs and combustion ashes have some similarities in their elemental/mineral compositions, we initially hypothesised that combustion ashes have a comparable ice nucleating efficiency to mineral dusts.

Combustion ashes can be classed into two groups: (1) bottom ashes – which are mainly the mineral remains of a complete combustion process, and (2) fly ashes – ash particles that are primarily emitted during combustion processes with further contributions from or the smelting of metallurgical materials, sometimes directly into the atmosphere (Adriano et al., 1980; USEPA, 2012; Hu et al., 2013). While coal is a major source of fly ash in the atmosphere, biomass burning, wildfires, and domestic combustion dominate the bottom ash emissions (Raison et al., 1985; Certini, 2005).

Coal fly ash is one of the major by-products of coal combustion from both household and power plants, used for the purpose of heating and generating electricity for industrial and domestic consumptions (ACCA, 2013; WCA, 2013; Mahlaba et al., 2012). There is increasing demand for coal to generate electricity around the globe. This has led to ~ 8000 million tonnes of coal being consumed daily in coal-fired power plants which are distributed all over the world (WCA, 2013). It is estimated that about 90 % of the fly ash is captured via different collection mechanisms such as electrostatic precipitators, fabric filters or bag houses, dust collectors, and other hybrid engineering systems like hot gas filtration systems (Bond et al., 2004; Wang et al., 2013; WCA, 2013). Nevertheless, sizeable quantities of these ash particles are emitted to the atmosphere as a result of inefficiencies associated with collection systems (e.g. electrostatic precipitators), and during transportation and storage of collected fly ash (Block and Dams, 1976).

Bottom ashes include ashes from the combustion of wood, other biomass, peat, coal and charcoal solid fuels and are produced during wildfires or bush-burning (agricultural practices) (Pereira and Úbeda, 2010), as well as in domestic and industrial settings (Chimenos et al., 1999). Bottom ashes can be lofted into the atmosphere via the action of wind sometime after the fire as well as during combustion (see Fig. 1). Compositional analyses of various ash samples from different sources have been investigated

Ice nucleation by combustion ash particles at conditions relevant to mixed-phase clouds

N. S. Umo et al.

Title Page	
Abstract	Introduction
Conclusions	References
Tables	Figures
◀	▶
◀	▶
Back	Close
Full Screen / Esc	
Printer-friendly Version	
Interactive Discussion	



Ice nucleation by combustion ash particles at conditions relevant to mixed-phase clouds

N. S. Umo et al.

Title Page

Abstract

Introduction

Conclusions

References

Tables

Figures

◀

▶

◀

▶

Back

Close

Full Screen / Esc

Printer-friendly Version

Interactive Discussion



previously, and efforts have focused on the effect of these ashes on agricultural soils, applications in cement production and disposal methods (Adriano et al., 1980; Basumajumdar et al., 2005). However, little attention has been given to the potential effect of these particles on cloud properties when they are lofted into the atmosphere.

5 Combustion ash particles emitted may have direct and indirect impacts on the planet's climate analogous to other types of aerosol particles (Forster, 2007; Murray et al., 2012) (as illustrated in Fig. 1). Many studies have shown that particles in the atmosphere such as mineral dust, soot, volcanic ash, pollen, fungi, and bacteria are INPs (Murray et al., 2012; Hoose and Möhler, 2012). Nevertheless, it is not known at
10 present if combustion ashes nucleate ice.

There are some indications that combustion ashes could be important INPs. Recently, several tens of percent of ice crystal residues from both prescribed burns and wildfires were carbonaceous-mineral and mineral-oxide mixed particles (McCluskey et al., 2014). It is possible that the inorganic mineral particles may have come from the combustion ash components of the fires. This is in contrast to Schnell et al. (1976) who
15 conducted an airborne study of INPs in a coal-fired power plant plume. They showed that plume particles did not act as INPs between -10 and -20 °C in the deposition or condensation mode, as no difference was observed between the background air and the plume. Conversely, a study on plume particles at a higher supersaturation with re-
20 spect to ice showed an enhancement, by a factor of two, in the number of INPs in the plume when compared to natural aerosols (Parungo et al., 1978). In summary, these studies indicated that fly ash has some ice nucleating potential, but there is no quantitative laboratory study of ice nucleation by combustion ashes in the immersion mode.

In this study, we first systematically characterized four types of combustion ashes obtained at well-defined conditions. We then quantify the ice nucleation activities of
25 these particles in the immersion mode.

2 Sources and generation of combustion ashes

In order to study ashes with a range of compositions representative of typical combustion ashes, we have generated ashes in both a controlled laboratory environment and a domestic setting, as well as obtaining fly ash from a large commercial power station.

5 Bottom ash samples from wood and coal were generated in the laboratory using a fixed grate multi-fuel stove rated at 6.5 kW (BS EN 13240:2001 and A2:2004), which is used for efficient burning of solid fuels. The solid fuel was lit by using a commercially available standard firelighter and it burned at relatively low temperature ($\sim 300^\circ\text{C}$). This temperature is more typical of domestic stoves and wildfires and contrasts with
10 high-temperature combustion systems in power plants ($\sim 1000^\circ\text{C}$ and above). The ash samples were collected after the combustion process from the ash pan fixed at the bottom of the stove.

Wood solid fuel used in generating the bottom ash samples was a standard commercially available domestic fuel, while the coal solid fuel was also a domestic fuel which
15 originated in Poland. Both solid fuels used for this study are representative fuels used for heating and cooking in many households in Europe and around the world.

Domestic bottom ashes were obtained in a similar way to wood and coal bottom ashes but from a stove in a typical household in Leeds, UK. The stove used here was a type approved by DEFRA (Department for Environment, Food & Rural Affairs) for use
20 in smoke control areas, hence, typical of modern domestic stoves with similar standard as the one mention earlier. The materials burned to obtain the domestic ash were unspecified soft and hard woods, with a few pieces of newsprint sheet used to ignite the solid fuel. Before the fire was set up, previous debris from the stove was cleaned out from the fireplace to avoid cross-contamination by previous ashes.

25 Coal fly ash (hereafter referred to as CFA) used in this study was fly ash released during coal combustion process in a typical large coal-fired power plant. The CFA sample used here was collected from an electrostatic precipitator, which is used to trap these particles to avoid their direct emission into the atmosphere. It should be pointed

Ice nucleation by combustion ash particles at conditions relevant to mixed-phase clouds

N. S. Umo et al.

Title Page

Abstract

Introduction

Conclusions

References

Tables

Figures



Back

Close

Full Screen / Esc

Printer-friendly Version

Interactive Discussion

out that, fly ashes can escape into the atmosphere if not effectively trapped or if inefficient handling methods are applied during its transport, disposal and storage as discussed in Sect. 1 (Buhre et al., 2005).

3 Preparation of ash suspension and freezing experiments

Suspensions containing CFA, wood, domestic, and coal bottom ashes were prepared by suspending a known mass of a specific combustion ash in a known mass of ultra-pure water (18.2 MΩ cm resistivity, TOC < 10 ppb) obtained from MilliQ Integral System (Millipore Water Purifier, USA). The suspension was placed in an ultra-sonic bath (Fisherbrand FB 15050 (S30)) for about 10 min and then stirred continuously for ~ 24 h to break down ash aggregates before carrying out freezing experiments.

We used two distinct experimental systems for the freezing experiments – the micro-litre Nucleation by Immersed Particles Instrument (μL-NIPI) and its nano-litre version (nL-NIPI). Both μL-NIPI and nL-NIPI are drop freezing experimental set-ups and have been described and used previously (Murray et al., 2010a; Broadley et al., 2012; Atkinson et al., 2013; O’Sullivan et al., 2014; Murray et al., 2011; Whale et al., 2014). Here, only a brief description of the procedure is presented: for experiments with nL-NIPI, ash-containing droplets were obtained by nebulizing the ash suspension onto a hydrophobic glass slide (12 mm, HR3-277, Hampton Research, USA), and placed on a cold stage. The stage was cooled with liquid nitrogen while the freezing temperatures, video and corresponding times, were recorded using a LabVIEW programme. Later, the video of the freezing droplets was analysed manually to yield the freezing temperature and size of each droplet.

For experiments with μL-NIPI, the droplets (1.00±0.025 μL) were directly placed onto a hydrophobic glass slide (22 mm diameter) using a Picus BIOHIT electronic pipette (Sartorius Ltd, UK). The glass slide was placed on a cold plate that was cooled by a Stirling cryocooler (Grant Asymptote EF600 instrument). Temperature uncertainty for μL-NIPI and nL-NIPI cold-stages are reported as ±0.4 °C and ±0.2 °C, respectively

Ice nucleation by combustion ash particles at conditions relevant to mixed-phase clouds

N. S. Umo et al.

Title Page

Abstract

Introduction

Conclusions

References

Tables

Figures



Back

Close

Full Screen / Esc

Printer-friendly Version

Interactive Discussion



(O'Sullivan et al., 2014; Atkinson et al., 2013; Whale et al., 2014). All results obtained from these set-ups are presented and discussed in Sect. 5.

4 Characterization of combustion ash samples

To ascertain the compositions of the combustion ashes, we employed a range of techniques to characterize the physical and the chemical properties of the ash samples. We measured their morphologies, surface areas, particle size distributions, and mineralogy, as reported in the following sub-sections.

4.1 Surface areas and morphology of ash particles

The ash particles were first size-segregated to $\leq 40 \mu\text{m}$ diameter by using test sieves and a sieve shaker (Endecotts M100, UK; ISO 9001 certified). Four 100 mm diameter test sieves, with mesh sizes of 71, 63, 55 and $50 \mu\text{m}$ were stacked above the $40 \mu\text{m}$ test sieve. The bottom ash particles passed through the $40 \mu\text{m}$ test sieve with ease indicating that at least two dimensions of the particles were smaller than $40 \mu\text{m}$. A fraction of the CFA particles were larger than $40 \mu\text{m}$ and did not pass through the sieve. The sieved ash samples were then used for all characterization processes reported here.

The specific surface areas (SSA) obtained from BET measurements of CFA and the bottom ashes are shown in Table 1. The SSAs of the ashes were measured following a standard Brunauer–Emmet–Teller (BET) nitrogen gas adsorption method (Gregg and Sing, 1982). We used an accelerated surface area and porosimetry system (Micromeritics ASAP 2020 Analyser, UK) for the measurements. Ash samples were degassed at about 120°C for 3 h prior to BET analyses.

Generally, the bottom ashes showed larger SSAs compared to CFA, with coal bottom ash particles having the largest SSA ($8.86 \text{ m}^2 \text{ g}^{-1}$). The observed variation in SSAs of the fly ash and that of bottom ashes are related to their different morphologies which

**Ice nucleation by
combustion ash
particles at
conditions relevant to
mixed-phase clouds**

N. S. Umo et al.

Title Page

Abstract

Introduction

Conclusions

References

Tables

Figures



Back

Close

Full Screen / Esc

Printer-friendly Version

Interactive Discussion



are due to different mechanisms by which the two ash types were generated (Buhre et al., 2005; Fenelonov et al., 2010).

The morphology of the combustion ash particles was also explored to see how this may influence their ice nucleation activities. A field emission gun (FEG – LEO 1530)

Scanning Electron Microscopy (SEM) instrument was used to investigate the surface properties of the ash particles; we looked at the surface morphology and the shapes of the ash particles. The SEM images of the ashes are shown in Fig. 2. From all the ashes investigated, only CFA showed spherical particles (Fig. 2a), similar to those in previous studies (Del Monte and Sabbioni, 1984; Nyambura et al., 2011; Flanders, 1999; Li and Shao, 2009); while the other ash samples had irregular shapes and tended to form aggregates.

The spherical shape of CFA particles is attributed to the formation mechanism of these particles as discussed previously by Fenelonov et al. (2010). Some CFA particles formed hollow spheres, which are referred to as cenospheres, and some of these hollow particles may be filled up by smaller-sized CFA particles and are referred to as plerospheres. High combustion temperatures and expansion of gas pockets are required for the formation of cenospheres, which is consistent with the production of this fly-ash in a commercial power station. The average diameter of CFA particles based on the SEM images was measured by using Image J[®] software as $\sim 5 \mu\text{m}$.

Wood bottom ash particles showed irregular shapes and aggregated particles as shown in Fig. 2b, but generally smaller in size compared to the CFA particles. Domestic bottom ash particles were highly agglomerated and asymmetrical shaped as shown in Fig. 2c, again, smaller than CFA particles but within the same size range as wood bottom ash particles (Fig. 2b). Domestic and wood bottom ashes were generated in similar combustion conditions and a similar fuel source; hence, they present similar particle morphologies. The SEM images of coal bottom ash particles (Fig. 2d) show that they were highly agglomerated and comprised smaller particles than CFA in spite of having a similar fuel source (coal), although formed under different combustion con-

Ice nucleation by combustion ash particles at conditions relevant to mixed-phase clouds

N. S. Umo et al.

Title Page

Abstract

Introduction

Conclusions

References

Tables

Figures



Back

Close

Full Screen / Esc

Printer-friendly Version

Interactive Discussion



ditions. Owing to the irregular shapes of all the bottom ash samples, it was not possible to estimate mean particle sizes from the SEM images.

4.2 Size distribution of combustion ash particles

We measured the particle size distribution for the combustion ash particles with a Malvern Mastersizer 2000E laser diffraction instrument that uses Mie theory to estimate the equivalent volume of the particles (Malvern, 2012; De Boer et al., 2002). A refractive index of 1.62 and absorption value of 1.0 was used for CFA and coal bottom ash based on suggestions by Jewell and Rathbone (2009). For wood and domestic bottom ashes, we used a refractive index of 1.65 and an absorption value of 0.1 because of their higher calcite content ($> 10\%$, see Table 2) (Jewell and Rathbone, 2009). The results in Fig. 3 are size distributions for ash suspensions agitated and stirred in the same way as for the ice nucleation experiments. From these measurements, we report an average volume diameter of $\sim 10\ \mu\text{m}$ for CFA while that of the bottom ashes is $\sim 8\ \mu\text{m}$ (Fig. 3).

4.3 Mineralogical analyses and elemental compositions of combustion ashes

The mineral compositions of the combustion ashes were analysed with an X-ray powder diffractometer (Bruker D8 Advance) and the results are reported in Table 2. The procedure using the same instrument has been described previously (Atkinson et al., 2013; Broadley et al., 2012; O'Sullivan et al., 2014).

The results showed variability in the mineral compositions of each ash type, but the proportions of major minerals such as quartz, calcite, haematite and magnetite were similar to biomass ash (Vassilev et al., 2013a, b; Misra et al., 1993). Quartz and haematite are also present in natural desert dust samples, but the ash samples used here are distinct from typical desert dusts in that they do not contain measurable amounts of clay and feldspar minerals. Another important distinction from desert dusts is that combustion ash samples contain 24 to 75% amorphous materials. Mullite

Ice nucleation by combustion ash particles at conditions relevant to mixed-phase clouds

N. S. Umo et al.

Title Page

Abstract

Introduction

Conclusions

References

Tables

Figures

◀

▶

◀

▶

Back

Close

Full Screen / Esc

Printer-friendly Version

Interactive Discussion



(Al₆Si₂O₁₃) was detected in CFA and coal bottom ash but not in other bottom ashes studied; and is characteristic of coal deposits. Generally, higher concentrations of calcite and gypsum were found in bottom ashes compared to the CFA which was generated at high temperatures.

Focusing on the CFA used this study, we found that its mineral composition (Table 2) was similar to the mineralogy of CFAs from different sources and locations. For example, the X-ray Diffraction (XRD) mineralogy for CFA in this study was found to be similar to CFA obtained from Sasol in South Africa (Nyambura et al., 2011). In addition, the amorphous content of the South African CFA (65%) was similar to that of the bulk sample used here (63%). Also, a study of CFAs from five separate power plants in the USA showed similar mineral compositions (ACAA, 2012). Previously, it has been reported that over 90% of CFA contain silicon-, aluminium-, calcium- and iron-based minerals (EPRI, 2010); this is consistent with the XRD and Energy dispersive X-ray spectroscopy (EDX) results obtained for our CFA. In general, fly ashes from large power plants are not strongly varied and our results for its ice nucleating abilities are therefore representative of coal power stations around the globe.

EDX analyses were carried out to study the elemental composition of individual ash particles. This was achieved using an EDX instrument (XMax 80 mm² by Oxford Instruments, UK), which was coupled to the SEM instrument. The key elements found in the CFA EDX spectra are shown in Fig. 4. Based on the locations scanned, principal elements found were Al, Si, Fe, O, and C. These elements are the major components of the minerals identified by the XRD. This result agrees with literature EDX spectra of ultra-fine ash particles, which is reported to comprise high levels of Ca, Si, and Fe (Chen et al., 2005). Although, carbon (C) showed a high count in the EDX spectra, it is not part of the major minerals listed; it could be a major component of CFA's amorphous composition. The elemental composition of coal bottom ash was similar to that of CFA but with a higher count for Ca (EDX spectra not shown).

The EDX spectra for wood and domestic bottom ashes identified the elements: C, O, Ca, Si, Mn, Fe, Mg, S, Na and K. High counts were observed for C, O, Mg, K and Ca

Ice nucleation by combustion ash particles at conditions relevant to mixed-phase clouds

N. S. Umo et al.

Title Page

Abstract

Introduction

Conclusions

References

Tables

Figures



Back

Close

Full Screen / Esc

Printer-friendly Version

Interactive Discussion



(spectra not shown). Potassium (K) is frequently found in combustion particles coming from wood fuel (Jenkins et al., 1998). From the XRD, the mineralogy of both wood and domestic bottom ashes shows that $\text{CaCO}_3/\text{CaSO}_4$ and SiO_2 are the major components. Therefore, high elemental contents of Ca and O are from the calcite/gypsum minerals found in them. Although SiO_2 is a major mineral also present in the ash, the amount of Si was substantially lower. It is possible that the location (or particle) where the EDX scanned did not contain quartz in a significant proportion. Overall, the elements identified were consistent with the mineralogy established by the XRD.

5 Results and discussion – ice nucleation by combustion ash samples

In this section, we present and discuss the results obtained from the freezing experiments on combustion ash particles.

5.1 Droplet freezing results

The results from the μL -NIPI freezing experiments with ash are shown in Fig. 5 and are compared with the average of 23 freezing experiments with ultra-pure water. In all cases, droplets containing combustion ash samples froze at warmer temperatures than ultra-pure water indicating that combustion ashes are capable of nucleating ice heterogeneously in the immersion mode.

The results of the nL-NIPI droplet freezing experiments are shown in Fig. 6. In these experiments the majority of the nanolitre-volume droplets of pure water containing no ash froze below -36°C , consistent with homogeneous nucleation reported by Murray et al. (2010a) and Riechers et al. (2013). This allows us to study ice nucleation by combustion ashes to lower temperatures than possible in the microlitre experiments. Inclusion of ash in these droplets causes them to freeze at warmer temperatures than in the pure water experiments, which indicates that the ash particles also nucleate ice in temperature range not accessible to the μL -NIPI experiment.

Ice nucleation by combustion ash particles at conditions relevant to mixed-phase clouds

N. S. Umo et al.

Title Page

Abstract

Introduction

Conclusions

References

Tables

Figures

◀

▶

◀

▶

Back

Close

Full Screen / Esc

Printer-friendly Version

Interactive Discussion



In these experiments droplets were generated by nebulizing 0.1 wt% aqueous suspensions of ash and collecting nanolitre droplets on a glass slide. As a result there was a very broad droplet size distribution (20–450 μm , diameter), unlike in the $\mu\text{L-NIPI}$ experiments where the droplets were of almost identical size. Importantly, there were also significant differences in droplet size distribution between experiments. Hence, the fraction frozen plots for each individual experiment in Fig. 6 are for a different droplet size distribution and cannot be directly compared. When the distribution was made up of smaller droplets, and therefore less surface area per droplet, the freezing temperatures are lower and vice versa. In order to quantitatively compare data from different runs on the nL-NIPI and also compare data from the nL-NIPI and $\mu\text{L-NIPI}$ experiments we need to normalise the probability of nucleation to the surface area per droplet.

5.2 The ice nucleation efficiency of combustion ashes

In order to describe the ice nucleating abilities of the different combustion ashes investigated, a singular model was adopted, which describes the cumulative number of active sites (n_s) which nucleate ice on cooling to a characteristic temperature (T) expressed per unit surface area of combustion ash. This model has been used in many ice nucleation studies to describe the ice nucleating efficiencies of particles, and detailed description of the model has also been given in (Vali, 1971; Broadley et al., 2012; Murray et al., 2012; Niedermeier et al., 2010; Hoose and Möhler, 2012; Murray et al., 2011; Atkinson et al., 2013; O’Sullivan et al., 2014; Vali, 2014). n_s is defined as:

$$n_s(T) = -\ln(1 - f_{\text{ice}}(T))\sigma^{-1} \quad (1)$$

where f_{ice} is the fraction of frozen droplets, which we implicitly assume is equal to the probability of a droplet being frozen at T , and σ is the surface area of the particles per droplet. The value of σ is determined from the SSA reported in Table 1 together with the mass fraction of the original suspension and the droplet volume.

For the $\mu\text{L-NIPI}$ some of the fraction frozen curves for droplets containing ash overlap in temperature range with the background freezing in pure water. In the past $\mu\text{L-NIPI}$

Ice nucleation by combustion ash particles at conditions relevant to mixed-phase clouds

N. S. Umo et al.

Title Page

Abstract

Introduction

Conclusions

References

Tables

Figures

◀

▶

◀

▶

Back

Close

Full Screen / Esc

Printer-friendly Version

Interactive Discussion



results have only been quoted above a threshold temperature above which the background is negligible (Atkinson et al., 2013; O’Sullivan et al., 2014; Whale et al., 2014). Here we use a method to subtract of the background INP concentration and determine n_s to lower temperatures. In this method, the cumulative INP concentration (INP per unit volume) for the background (K_{bgd}) is subtracted off the cumulative INP concentration for the ash containing samples (K_{tot}).

$$K_{\text{het}} = K_{\text{tot}} - K_{\text{bgd}} \quad (2)$$

Here the K_{het} is the cumulative INP concentration due to the heterogeneous freezing by the ash samples. K_{bgd} is obtained from the fit to the experimental data of ultra-pure water given as:

$$K_{\text{bgd}} = \exp(mT + d) \quad (3)$$

where m (-0.44 ± 0.01) and d (-5.08 ± 0.24) are the gradient and intercept of the fit, respectively. K_{het} is then used to determine n_s as shown in Eq. (4). The determination of K and its relationship with n_s is set out by Murray et al. (2012) and Vali (2014).

$$n_s(T) = [-\ln(1 - F_{\text{tot}})V^{-1} - \exp(mT + d)]C^{-1}A^{-1} \quad (4)$$

where C is the concentration of samples in the droplet (g) and A is the specific surface area (cm^2g^{-1}). Uncertainties in K_{bgd} , droplet volume and specific surface area are propagated to estimate uncertainty in n_s . A comparable methodology was recently employed by Hader et al. (2014) to correct for background freezing in similar experiments for heterogeneous freezing by pollen.

For the nL-NIPI results the determination of n_s needed to take into account the broad size distribution of the droplets (20–450 μm diameter). In the past, we have used a method where we bin droplets into narrow size ranges and then apply Eq. (1) using the average surface area per droplet (Murray et al., 2010a), but here we used a moving

average method. The total surface area was summed over all liquid droplets and modified as droplets freeze to obtain an accumulative nucleation sites density (n_s). This method is similar to that used by Vali (1971).

Values of n_s for each combustion ash sample from both μL - and nL-NIPI experiments are presented in Fig. 7. The n_s distribution of results from both μL - and nL-NIPI experiments showed good agreement even though the surface area per droplet varied by six orders of magnitude. The agreement between data from experiments with vastly different droplet volumes and therefore vastly different surface areas per droplet is consistent with the probability of nucleation scaling with surface area.

In the determination of n_s from nL-NIPI results we assumed that the background INP concentrations were negligible. In general, this appears to be a reasonable approximation, but it is possible that for runs employing the largest droplets ($> 100 \mu\text{m}$) there may have been a significant number of background INPs present in the droplets. Accordingly, this could lead to slight deviations for the highest temperature nL-NIPI n_s values when compared to the equivalent μL -NIPI n_s values. Note that some pure water droplets freeze above -36°C (Fig. 6). Even with this potential contribution of background INP in some nL-NIPI experiments, the agreement between the various experiments shown in Fig. 7 is reasonable.

Inspection of the various plots in Fig. 7 reveals a striking difference in temperature dependence of n_s between the CFA and the bottom ash samples. While CFA is well described by a log exponential fit, wood and coal bottom ashes were well described by a log linear relationship and domestic ash was better fitted by a log polynomial fit. The fitted parameterizations for each data set are listed in Table 3. The shape of the CFA n_s curve is reminiscent of bacterial or fungal INP in which there is an onset-like behaviour where the number of active sites increases rapidly with temperature, followed by a much shallower increase in active sites at lower temperature. The steep increase in n_s around -17°C in CFA shows that the sites active around this temperature are less diverse than those in the bottom ash samples. In contrast, the bottom ash samples have measurable n_s to temperatures well above -17°C .

Ice nucleation by combustion ash particles at conditions relevant to mixed-phase clouds

N. S. Umo et al.

Title Page

Abstract

Introduction

Conclusions

References

Tables

Figures

◀

▶

◀

▶

Back

Close

Full Screen / Esc

Printer-friendly Version

Interactive Discussion



Ice nucleation by combustion ash particles at conditions relevant to mixed-phase clouds

N. S. Umo et al.

Title Page

Abstract

Introduction

Conclusions

References

Tables

Figures

◀

▶

◀

▶

Back

Close

Full Screen / Esc

Printer-friendly Version

Interactive Discussion

In Fig. 8 we compare the $n_s(T)$ of the four ash samples (mineral dust n_s values are also included in this plot, but are discussed in Sect. 5.3). Inspection of Fig. 8 shows that CFA is more efficient at nucleating ice between about -17°C and -27°C than the bottom ashes, but its activity falls away very rapidly above -17°C . The bottom ash samples are more similar to one another, but there is a trend with the coal ash being least active and the wood ash being most active between $\sim -12^\circ\text{C}$ and the homogeneous limit. These differences must in some way be related to the fuel, combustion temperature, ash composition and ash morphology. In terms of morphology and generation conditions, CFA is very different to the bottom ashes. As shown earlier (Fig. 2), CFA was made up of spherical particles whereas the bottom ashes were irregular-shaped particles. Moreover, CFA was produced in a high temperature combustion system, $1500\text{--}1900^\circ\text{C}$, in contrast to the bottom ashes which were generated at about $\sim 300^\circ\text{C}$ (see Sect. 2.1). CFA was produced at a very high temperature in a limited oxygen condition, the bottom ashes were generated in a sufficient oxygen supply system. These combustion conditions can affect the chemistry and composition of the particles (Misra et al., 1993), and apparently also influence ice nucleating abilities. However, the particular reason why CFA has a distinct nucleation spectrum remains a subject for further investigation.

5.3 Comparison of ice nucleation activities of combustion ashes to INPs with varied mineralogies

Combustion ashes have some similarities with mineral dusts from deserts in terms of their composition; hence, we have compared literature values of n_s for various mineral and desert dusts in Fig. 8. For mineral-based INPs, the observed variations in their ice nucleation activities have been linked to differences in their mineralogies (Atkinson et al., 2013; Augustin-Bauditz et al., 2014). In particular, feldspars have been identified as the most active mineral group present in typical desert dusts followed by quartz with the clays only becoming similarly active at much lower temperatures (Atkinson et al., 2013).

Ice nucleation by combustion ash particles at conditions relevant to mixed-phase clouds

N. S. Umo et al.

Title Page

Abstract

Introduction

Conclusions

References

Tables

Figures

◀

▶

◀

▶

Back

Close

Full Screen / Esc

Printer-friendly Version

Interactive Discussion



ities of the ashes generated from different fuels and under different conditions. Ashes are composed of silicates and might therefore be expected to have some similarities in their ice nucleating ability to mineral dusts, but the nucleating efficiency (n_s) of the ashes is lower than that of desert dusts reported in the literature. This is probably because the ashes do not contain the highly ice active feldspars, which are present in desert dusts. However, the ice nucleation activities of combustion ashes may be influenced by the presence of quartz, but this suggestion needs further investigation.

At present it is not possible to assess the potential contribution of ashes to the INP loading of the earth's atmosphere due to a lack of data on their atmospheric abundance. There is a lack of information on the abundance of combustion ashes in the atmosphere, in part, because these ashes are difficult to distinguish from mineral dusts and therefore tend to be counted together with mineral dust particles. There is only one study we are aware of where the contribution of fly ash to ice crystal residues was estimated (DeMott, 2003). This study was for cirrus cloud conditions rather than lower altitude mixed phase clouds, hence may not be directly relevant, but nevertheless illustrates the potential importance of combustion ash INP. Single particle mass spectrometry was used to show that 33% of the ice crystal residues were “mineral dust/fly ash” and they then used electron microscopy to show that 20% of the particles in this category had a high degree of sphericity which indicated that they were fly ash. This is intriguing because ~7% of the ice crystal residues were therefore fly ash. In addition, it should also be noted that their electron microscopy technique could not identify aerosolised irregular shaped bottom ash particles; hence, 7% is probably a lower limit for the contribution of combustion ash to the measurements of DeMott et al. (2003).

As a follow up to this research, we propose that measurements are needed to constrain the abundance of combustion ashes in the atmosphere. A clear distinction needs to be made between mineral dust, fly ashes, and volcanic ashes by potentially using methods like magnetisation and coercive field factors (Flanders, 1999; Xie and Dearing, 1999). The coercive field factor gives an indication of the percentage of fly ash that

Ice nucleation by combustion ash particles at conditions relevant to mixed-phase clouds

N. S. Umo et al.

Title Page

Abstract

Introduction

Conclusions

References

Tables

Figures

◀

▶

◀

▶

Back

Close

Full Screen / Esc

Printer-friendly Version

Interactive Discussion



is airborne in relation to the total amount of magnetic material that is airborne. Other methods are isotopic labelling and back trajectories correction. Isotopic labelling can be used during measurements by matching the spectra of the minerals in the atmosphere with the known isotopes characteristic of the possible sources of the measured particles. Back trajectory involves resolving the emission sources of combustion ashes and comparing to the emission route for natural dusts.

To ascertain the contribution of combustion ashes to tropospheric INPs and its impact on clouds, we also propose that further studies should focus on quantifying the effect of atmospheric processing and its implications for their ice nucleation abilities. This can give relevant information on the impact of freshly emitted and aged combustion ash particles. Lastly, the impact of these ashes on localized clouds (i.e. in the region of ash emission) may also be of interest for future assessment. In summary, we suggest that ice nucleation by combustion ashes could have an important impact on clouds and consequently on climate, but more work is needed.

Acknowledgements. The authors are grateful to Edward Mitchell for his assistance in generating some of the ash samples and James (Jim) McQuaid for helpful discussions on atmospheric measurements of aerosol particles. We thank John N. Ward, Chairman of the American Coal Ash Association's Government Relations Committee, for helpful discussions on coal fly ash production. This project was funded by the European Research Council (FP7, 240449 ICE) and the Natural Environment Research Council (NE/I020059/1, NE/I013466/1, NE/H001050/1, NE/K004417/1). NSU acknowledges the Niger Delta Development Commission (NDDC) in Nigeria for the financial assistance during his PhD studies (NDDC/DEHSS/2010PGFS/AK/011).

References

- ACAA: Coal Ash Material Safety – a Health Risk-Based Evaluation of USGS Coal Ash Data from Five US Power Plants, American Coal Ash Association, Chelmsford, MA, 2012.
- ACCA: Coal Combustion Products Production and Use Statistics by American Coal Ash Association, Advancing The Management and Use of Coal Combustion Products, Michigan, 2013.

Ice nucleation by combustion ash particles at conditions relevant to mixed-phase clouds

N. S. Umo et al.

Title Page

Abstract

Introduction

Conclusions

References

Tables

Figures

◀

▶

◀

▶

Back

Close

Full Screen / Esc

Printer-friendly Version

Interactive Discussion

- Adriano, D. C., Page, A. L., Elseewi, A. A., Chang, A. C., and Straughan, I.: Utilization and disposal of fly ash and other coal residues in terrestrial ecosystems: a review, *J. Environ. Qual.*, 9, 333–344, 1980.
- Ansmann, A., Tesche, M., Seifert, P., Althausen, D., Engelmann, R., Fruntke, J., Wandinger, U.,
5 Mattis, I., and Müller, D.: Evolution of the ice phase in tropical altocumulus: sa-
mum lidar observations over cape verde, *J. Geophys. Res.-Atmos.*, 114, D17208,
doi:10.1029/2008JD011659, 2009.
- Atkinson, J. D., Murray, B. J., Woodhouse, M. T., Whale, T. F., Baustian, K. J., Carslaw, K. S.,
Dobbie, S., O'Sullivan, D., and Malkin, T. L.: The importance of feldspar for ice nucleation by
10 mineral dust in mixed-phase clouds, *Nature*, 498, 355–358, 2013.
- Augustin-Bauditz, S., Wex, H., Kanter, S., Ebert, M., Niedermeier, D., Stolz, F., Prager, A.,
and Stratmann, F.: The immersion mode ice nucleation behavior of mineral dusts:
a comparison of different pure and surface modified dusts, *Geophys. Res. Lett.*,
doi:10.1002/2014GL061317, 2014.
- 15 Basumajumdar, A., Das, A. K., Bandyopadhyay, N., and Maitra, S.: Some studies on the reac-
tion between fly ash and lime, *B. Mater. Sci.*, 28, 131–136, 2005.
- Baustian, K. J., Cziczo, D. J., Wise, M. E., Pratt, K. A., Kulkarni, G., Hallar, A. G., and Tol-
bert, M. A.: Importance of aerosol composition, mixing state, and morphology for heteroge-
neous ice nucleation: A combined field and laboratory approach, *J. Geophys. Res.-Atmos.*,
20 117, D06217, doi:10.1029/2011JD016784, 2012.
- Block, C. and Dams, R.: Study of fly ash emission during combustion of coal, *Environ. Sci.
Technol.*, 10, 1011–1017, 1976.
- Bond, T. C., Streets, D. G., Yarber, K. F., Nelson, S. M., Woo, J. H., and Klimont, Z.:
A technology-based global inventory of black and organic carbon emissions from combus-
25 tion, *J. Geophys. Res.-Atmos.*, 109, D14203, doi:10.1029/2003JD003697, 2004.
- Bond, T. C., Doherty, S. J., Fahey, D. W., Forster, P. M., Berntsen, T., DeAngelo, B. J., Flanner,
M. G., Ghan, S., Kärcher, B., Koch, D., Kinne, S., Kondo, Y., Quinn, P. K., Sarofim, M. C.,
Schultz, M. G., Schulz, M., Venkataraman, C., Zhang, H., Zhang, S., Bellouin, N., Guttikunda,
S. K., Hopke, P. K., Jacobson, M. Z., Kaiser, J. W., Klimont, Z., Lohmann, U., Schwarz,
30 J. P., Shindell, D., Storelvmo, T., Warren, S. G., and Zender, C. S.: Bounding the role of
black carbon in the climate system: a scientific assessment, *J. Geophys. Res.-Atmos.*, 118,
5380–5552, 2013.

Ice nucleation by combustion ash particles at conditions relevant to mixed-phase clouds

N. S. Umo et al.

Title Page

Abstract

Introduction

Conclusions

References

Tables

Figures

◀

▶

◀

▶

Back

Close

Full Screen / Esc

Printer-friendly Version

Interactive Discussion



- Broadley, S. L., Murray, B. J., Herbert, R. J., Atkinson, J. D., Dobbie, S., Malkin, T. L., Condliffe, E., and Neve, L.: Immersion mode heterogeneous ice nucleation by an illite rich powder representative of atmospheric mineral dust, *Atmos. Chem. Phys.*, 12, 287–307, doi:10.5194/acp-12-287-2012, 2012.
- 5 Buhre, B. J. P., Hinkley, J. T., Gupta, R. P., Wall, T. F., and Nelson, P. F.: Submicron ash formation from coal combustion, *Fuel*, 84, 1206–1214, 2005.
- Certini, G.: Effects of fire on properties of forest soils: a review, *Oecologia*, 143, 1–10, 2005.
- Chen, H., Laskin, A., Baltrusaitis, J., Gorski, C. A., Scherer, M. M., and Grassian, V. H.: Coal fly ash as a source of iron in atmospheric dust, *Environ. Sci. Technol.*, 46, 2112–2120, 2012.
- 10 Chen, Y., Shah, N., Huggins, F. E., and Huffman, G. P.: Transmission electron microscopy investigation of ultrafine coal fly ash particles, *Environ. Sci. Technol.*, 39, 1144–1151, 2005.
- Chimeno, J. M., Segarra, M., Fernández, M. A., and Espiell, F.: Characterization of the bottom ash in municipal solid waste incinerator, *J. Hazard. Mater.*, 64, 211–222, 1999.
- Cziczo, D. J., Murphy, D. M., Hudson, P. K., and Thomson, D. S.: Single particle measurements of the chemical composition of cirrus ice residue during crystal-face, *J. Geophys. Res.-Atmos.*, 109, D04201, doi:10.1029/2003JD004032, 2004.
- 15 Cziczo, D. J., Froyd, K. D., Hoose, C., Jensen, E. J., Diao, M., Zondlo, M. A., Smith, J. B., Twohy, C. H., and Murphy, D. M.: Clarifying the dominant sources and mechanisms of cirrus cloud formation, *Science*, 340, 1320–1324, 2013.
- 20 De Boer, A., Gjaltema, D., Hagedoorn, P., and Frijlink, H.: Characterization of inhalation aerosols: a critical evaluation of cascade impactor analysis and laser diffraction technique, *Int. J. Pharm.*, 249, 219–231, 2002.
- Del Monte, M. and Sabbioni, C.: Morphology and mineralogy of fly ash from a coal-fueled power plant, *Arch. Meteor. Geophys. B*, 35, 93–104, 1984.
- 25 Demott, P. J.: An exploratory-study of ice nucleation by soot aerosols, *J. Appl. Meteorol.*, 29, 1072–1079, 1990.
- Demott, P. J., Cziczo, D. J., Prenni, A. J., Murphy, D. M., Kreidenweis, S. M., Thomson, D. S., Borys, R., and Rogers, D. C.: Measurements of the concentration and composition of nuclei for cirrus formation, *P. Natl. Acad. Sci. USA*, 100, 14655–14660, 2003.
- 30 EPRI: Comparison of coal combustion products to other common materials: chemical characteristics, Electric Power Research Institute, 1020556, 21–26, 2010.

Ice nucleation by combustion ash particles at conditions relevant to mixed-phase clouds

N. S. Umo et al.

Title Page

Abstract

Introduction

Conclusions

References

Tables

Figures

◀

▶

◀

▶

Back

Close

Full Screen / Esc

Printer-friendly Version

Interactive Discussion



Fenelonov, V. B., Mel'gunov, M. S., and Parmon, V. N.: The properties of cenospheres and the mechanism of their formation during high-temperature coal combustion at thermal power plants, KONA, California, 1020556, 21–26, 2010.

Fitzpatrick, E. M., Jones, J. M., Pourkashanian, M., Ross, A. B., Williams, A., and Bartle, K. D.: Mechanistic aspects of soot formation from the combustion of pine wood, *Energ. Fuel.*, 22, 3771–3778, 2008.

Flanders, P. J.: Identifying fly ash at a distance from fossil fuel power stations, *Environ. Sci. Technol.*, 33, 528–532, 1999.

Forster, P., Ramaswamy, V., Artaxo, P., Bernsten, T., Betts, R., Fahey, D. W., Haywood, J., Lean, J., Lowe, D. C., Myhre, G., Nganga, J., Prinn, R., Raga, G., Schulz, M., and Van Dorland, R.: Changes in atmospheric constituents and in radiative forcing, in: *Climate Change 2007: the Physical Science Basis*, contribution of Working Group I to the Fourth Assessment Report of the Intergovernmental Panel on Climate Change, edited by: Solomon, S., Qin, D., Manning, M., Chen, Z., Marquis, M., Averyt, K. B., Tignor, M., and Miller, H. L., 28 pp., Cambridge University Press, Cambridge, UK, 2007.

Friedman, B., Zelenyuk, A., Beranek, J., Kulkarni, G., Pekour, M., Gannet Hallar, A., McCubbin, I. B., Thornton, J. A., and Cziczo, D. J.: Aerosol measurements at a high-elevation site: composition, size, and cloud condensation nuclei activity, *Atmos. Chem. Phys.*, 13, 11839–11851, doi:10.5194/acp-13-11839-2013, 2013.

Gregg, S. and Sing, K.: *Adsorption, Surface Area and Porosity*, Academic Press London, UK, 303 pp., 1982.

Hader, J. D., Wright, T. P., and Petters, M. D.: Contribution of pollen to atmospheric ice nuclei concentrations, *Atmos. Chem. Phys.*, 14, 5433–5449, doi:10.5194/acp-14-5433-2014, 2014.

Herbert, R. J., Murray, B. J., Whale, T. F., Dobbie, S. J., and Atkinson, J. D.: Representing time-dependent freezing behaviour in immersion mode ice nucleation, *Atmos. Chem. Phys.*, 14, 8501–8520, doi:10.5194/acp-14-8501-2014, 2014.

Hiranuma, N., Augustin-Bauditz, S., Bingemer, H., Budke, C., Curtius, J., Danielczok, A., Diehl, K., Dreischmeier, K., Ebert, M., Frank, F., Hoffmann, N., Kandler, K., Kiselev, A., Koop, T., Leisner, T., Möhler, O., Nillius, B., Peckhaus, A., Rose, D., Weinbruch, S., Wex, H., Boose, Y., DeMott, P. J., Hader, J. D., Hill, T. C. J., Kanji, Z. A., Kulkarni, G., Levin, E. J. T., McCluskey, C. S., Murakami, M., Murray, B. J., Niedermeier, D., Petters, M. D., O'Sullivan, D., Saito, A., Schill, G. P., Tajiri, T., Tolbert, M. A., Welti, A., Whale, T. F., Wright, T. P., and Yamashita, K.: A comprehensive laboratory study on the immersion freezing behavior of illite

Ice nucleation by combustion ash particles at conditions relevant to mixed-phase clouds

N. S. Umo et al.

Title Page

Abstract

Introduction

Conclusions

References

Tables

Figures

◀

▶

◀

▶

Back

Close

Full Screen / Esc

Printer-friendly Version

Interactive Discussion



NX particles: a comparison of seventeen ice nucleation measurement techniques, *Atmos. Chem. Phys. Discuss.*, 14, 22045–22116, doi:10.5194/acpd-14-22045-2014, 2014.

Hoose, C. and Möhler, O.: Heterogeneous ice nucleation on atmospheric aerosols: a review of results from laboratory experiments, *Atmos. Chem. Phys.*, 12, 9817–9854, doi:10.5194/acp-12-9817-2012, 2012.

Hu, W. W., Hu, M., Yuan, B., Jimenez, J. L., Tang, Q., Peng, J. F., Hu, W., Shao, M., Wang, M., Zeng, L. M., Wu, Y. S., Gong, Z. H., Huang, X. F., and He, L. Y.: Insights on organic aerosol aging and the influence of coal combustion at a regional receptor site of central eastern China, *Atmos. Chem. Phys.*, 13, 10095–10112, doi:10.5194/acp-13-10095-2013, 2013.

Jacobson, M. Z.: Effects of biomass burning on climate, accounting for heat and moisture fluxes, black and brown carbon, and cloud absorption effects, *J. Geophys. Res.-Atmos.*, 119, 8980–9002, doi:10.1002/2014JD021861, 2014.

Jenkins, B. M., Baxter, L. L., Miles Jr., T. R., and Miles, T. R.: Combustion properties of biomass, *Fuel Process. Technol.*, 54, 17–46, 1998.

Jewell, R. B. and Rathbone, R. F.: Optical properties of coal combustion byproducts for particle-size analysis by laser diffraction, *Coal Combustion and Gasification Products*, 1, 1–7, 2009.

Kamphus, M., Ettner-Mahl, M., Klimach, T., Drewnick, F., Keller, L., Cziczko, D. J., Mertes, S., Borrmann, S., and Curtius, J.: Chemical composition of ambient aerosol, ice residues and cloud droplet residues in mixed-phase clouds: single particle analysis during the Cloud and Aerosol Characterization Experiment (CLACE 6), *Atmos. Chem. Phys.*, 10, 8077–8095, doi:10.5194/acp-10-8077-2010, 2010.

Kireeva, E. D., Popovicheva, O. B., Persiantseva, N. M., Khokhlova, T. D., and Shonija, N. K.: Effect of black carbon particles on the efficiency of water droplet freezing, *Colloid J.*, 71, 353–359, 2009.

Kumai, M.: Snow crystals and the identification of the nuclei in the northern united-states of america, *J. Meteorol.*, 18, 139–150, 1961.

Li, J., Posfai, M., Hobbs, P. V., and Buseck, P. R.: Individual aerosol particles from biomass burning in southern Africa: 2, compositions and aging of inorganic particles, *J. Geophys. Res.-Atmos.*, 108, 8484, doi:10.1029/2002JD002310, 2003.

Li, W. and Shao, L.: Transmission electron microscopy study of aerosol particles from the brown hazes in northern China, *J. Geophys. Res.-Atmos.*, 114, D09302, doi:10.1029/2008JD011285, 2009.

**Ice nucleation by
combustion ash
particles at
conditions relevant to
mixed-phase clouds**

N. S. Umo et al.

Title Page

Abstract

Introduction

Conclusions

References

Tables

Figures

◀

▶

◀

▶

Back

Close

Full Screen / Esc

Printer-friendly Version

Interactive Discussion

dust particles – measurements and parameterization, *Atmos. Chem. Phys.*, 10, 3601–3614, doi:10.5194/acp-10-3601-2010, 2010.

Niemand, M., Möhler, O., Vogel, B., Vogel, H., Hoose, C., Connolly, P., Klein, H., Bingemer, H., Demott, P., Skrotzki, J., and Leisner, T.: A particle-surface-area-based parameterization of immersion freezing on desert dust particles, *J. Atmos. Sci.*, 69, 3077–3092, 2012.

Nyambura, M. G., Mugeru, G. W., Felicia, P. L., and Gathura, N. P.: Carbonation of brine impacted fractionated coal fly ash: implications for CO₂ sequestration, *J. Environ. Manage.*, 92, 655–664, 2011.

O'Sullivan, D., Murray, B. J., Malkin, T. L., Whale, T. F., Umo, N. S., Atkinson, J. D., Price, H. C., Baustian, K. J., Browse, J., and Webb, M. E.: Ice nucleation by fertile soil dusts: relative importance of mineral and biogenic components, *Atmos. Chem. Phys.*, 14, 1853–1867, doi:10.5194/acp-14-1853-2014, 2014.

Parungo, F., Ackerman, E., Proulx, H., and Pueschel, R.: Nucleation properties of fly ash in a coal-fired power-plant plume, *Atmos. Environ.*, 12, 929–935, 1978.

Pereira, P. and Úbeda, X.: Spatial distribution of heavy metals released from ashes after a wildfire, *J. Environ. Eng. Landsc.*, 18, 13–22, 2010.

Petters, M. D., Parsons, M. T., Prenni, A. J., Demott, P. J., Kreidenweis, S. M., Carrico, C. M., Sullivan, A. P., Mcmeeking, G. R., Levin, E., Wold, C. E., Collett, J. L., and Moosmuller, H.: Ice nuclei emissions from biomass burning, *J. Geophys. Res.-Atmos.*, 114, 148–227, doi:10.1029/2008JD011532, 2009.

Popovicheva, O., Kireeva, E., Persiantseva, N., Khokhlova, T., Shonija, N., Tishkova, V., and Demirdjian, B.: Effect of soot on immersion freezing of water and possible atmospheric implications, *Atmos. Res.*, 90, 326–337, 2008.

Posfai, M., Gelencser, A., Simonics, R., Arato, K., Li, J., Hobbs, P. V., and Buseck, P. R.: Atmospheric tar balls: particles from biomass and biofuel burning, *J. Geophys. Res.-Atmos.*, 109, D06213, doi:10.1029/2003JD004169, 2004.

Pósfai, M., Simonics, R., Li, J., Hobbs, P. V., and Buseck, P. R.: Individual aerosol particles from biomass burning in southern africa: 1. Compositions and size distributions of carbonaceous particles, *J. Geophys. Res.-Atmos.*, 108, 8483, doi:10.1029/2002JD002291, 2003.

Pratt, K. A., Demott, P. J., French, J. R., Wang, Z., Westphal, D. L., Heymsfield, A. J., Twohy, C. H., Prenni, A. J., and Prather, K. A.: In situ detection of biological particles in cloud ice-crystals, *Nat. Geosci.*, 2, 398–401, 2009.

**Ice nucleation by
combustion ash
particles at
conditions relevant to
mixed-phase clouds**

N. S. Umo et al.

Title Page

Abstract

Introduction

Conclusions

References

Tables

Figures

◀

▶

◀

▶

Back

Close

Full Screen / Esc

Printer-friendly Version

Interactive Discussion



- Pratt, K. A., Heymsfield, A. J., Twohy, C. H., Murphy, S. M., Demott, P. J., Hudson, J. G., Subramanian, R., Wang, Z., Seinfeld, J. H., and Prather, K. A.: In situ chemical characterization of aged biomass-burning aerosols impacting cold wave clouds, *J. Atmos. Sci.*, 67, 2451–2468, 2010.
- 5 Raison, R. J., Khanna, P. K., and Woods, P. V.: Mechanisms of element transfer to the atmosphere during vegetation fires, *Can. J. Forest Res.*, 15, 132–140, 1985.
- Richardson, M. S., DeMott, P. J., Kreidenweis, S. M., Cziczo, D. J., Dunlea, E. J., Jimenez, J. L., Thomson, D. S., Ashbaugh, L. L., Borys, R. D., Westphal, D. L., Casuccio, G. S., Lersch, T. L.: Measurements of heterogeneous ice nuclei in the western united states in spring-
10 time and their relation to aerosol characteristics, *J. Geophys. Res.-Atmos.*, 112, D02209, doi:10.1029/2006JD007500, 2007.
- Riechers, B., Wittbracht, F., Hutten, A., and Koop, T.: The homogeneous ice nucleation rate of water droplets produced in a microfluidic device and the role of temperature uncertainty, *Phys. Chem. Chem. Phys.*, 15, 5873–5887, 2013.
- 15 Schnell, R. C., Van Valin, C. C., and Pueschel, R. F.: Atmospheric ice nuclei: no detectable effects from a coal-fired powerplant plume, *Geophys. Res. Lett.*, 3, 657–660, 1976.
- Spracklen, D. V., Carslaw, K. S., Pöschl, U., Rap, A., and Forster, P. M.: Global cloud condensation nuclei influenced by carbonaceous combustion aerosol, *Atmos. Chem. Phys.*, 11, 9067–9087, doi:10.5194/acp-11-9067-2011, 2011.
- 20 Tobo, Y., DeMott, P. J., Hill, T. C. J., Prenni, A. J., Swoboda-Colberg, N. G., Franc, G. D., and Kreidenweis, S. M.: Organic matter matters for ice nuclei of agricultural soil origin, *Atmos. Chem. Phys.*, 14, 8521–8531, doi:10.5194/acp-14-8521-2014, 2014.
- USEPA: Coal-Clean Energy-US EPA, Washington DC and United States Environmental Protection Agency (USEPA), 2012.
- 25 Vali, G.: Quantitative evaluation of experimental results an the heterogeneous freezing nucleation of supercooled liquids, *J. Atmos. Sci.*, 28, 402–409, 1971.
- Vali, G.: Nucleation terminology, *J. Aerosol Sci.*, 16, 575–576, 1985.
- Vali, G.: Interpretation of freezing nucleation experiments: singular and stochastic; sites and surfaces, *Atmos. Chem. Phys.*, 14, 5271–5294, doi:10.5194/acp-14-5271-2014, 2014.
- 30 Vali, G., DeMott, P., Möhler, O., and Whale, T. F.: Ice nucleation terminology, *Atmos. Chem. Phys. Discuss.*, 14, 22155–22162, doi:10.5194/acpd-14-22155-2014, 2014.

**Ice nucleation by
combustion ash
particles at
conditions relevant to
mixed-phase clouds**

N. S. Umo et al.

[Title Page](#)[Abstract](#)[Introduction](#)[Conclusions](#)[References](#)[Tables](#)[Figures](#)[⏪](#)[⏩](#)[◀](#)[▶](#)[Back](#)[Close](#)[Full Screen / Esc](#)[Printer-friendly Version](#)[Interactive Discussion](#)

Vassilev, S. V., Baxter, D., Andersen, L. K., and Vassileva, C. G.: An overview of the composition and application of biomass ash. Part 1. Phase–mineral and chemical composition and classification, *Fuel*, 105, 40–76, 2013a.

Vassilev, S. V., Baxter, D., Andersen, L. K., and Vassileva, C. G.: An overview of the composition and application of biomass ash.: Part 2. Potential utilisation, technological and ecological advantages and challenges, *Fuel*, 105, 19–39, 2013b.

Wang, X., Williams, B. J., Wang, X., Tang, Y., Huang, Y., Kong, L., Yang, X., and Biswas, P.: Characterization of organic aerosol produced during pulverized coal combustion in a drop tube furnace, *Atmos. Chem. Phys.*, 13, 10919–10932, doi:10.5194/acp-13-10919-2013, 2013.

WCA: Coal Combustion Products Report, World Coal Association, London, 2013.

Westerling, A. L., Hidalgo, H. G., Cayan, D. R., and Swetnam, T. W.: Warming and earlier spring increase western US forest wildfire activity, *Science*, 313, 940–943, 2006.

Whale, T. F., Murray, B. J., O’Sullivan, D., Umo, N. S., Baustian, K. J., Atkinson, J. D., and Morris, G. J.: A technique for quantifying heterogeneous ice nucleation in microlitre supercooled water droplets, *Atmos. Meas. Tech. Discuss.*, 7, 9509–9536, doi:10.5194/amtd-7-9509-2014, 2014.

Williams, A., Jones, J. M., Ma, L., and Pourkashanian, M.: Pollutants from the combustion of solid biomass fuels, *Prog. Energ. Combust.*, 38, 113–137, 2012.

Xie, S. and Dearing, J. A.: Comment on “Identifying fly ash at a distance from fossil fuel power stations”, *Environ. Sci. Technol.*, 33, 4140–4140, 1999.

Zhang, Y., Schauer, J. J., Zhang, Y., Zeng, L., Wei, Y., Liu, Y., and Shao, M.: Characteristics of particulate carbon emissions from real-world chinese coal combustion, *Environ. Sci. Technol.*, 42, 5068–5073, 2008.

Ice nucleation by combustion ash particles at conditions relevant to mixed-phase clouds

N. S. Umo et al.

Title Page

Abstract

Introduction

Conclusions

References

Tables

Figures

◀

▶

◀

▶

Back

Close

Full Screen / Esc

Printer-friendly Version

Interactive Discussion

Table 1. Specific surface areas (SSA) of combustion ashes as measured by BET nitrogen gas adsorption method. All coal fly ash (CFA), wood, domestic, and coal bottom ashes were sieved to $\leq 40 \mu\text{m}$ before the measurement except CFA (bulk). CFA (bulk) denotes a raw CFA sample as obtained from an electrostatic precipitator of a coal-fired power plant. All data reported here were measured from a five-point adsorption isotherm with correlation coefficient of ≥ 0.9975 . The uncertainties in the measurements are indicated on a separate column.

Samples	BET ($\text{m}^2 \text{g}^{-1}$)	Uncertainty ($\text{m}^2 \text{g}^{-1}$)
coal fly ash (bulk)	1.85	0.04
coal fly ash (sieved to $\leq 40 \mu\text{m}$)	2.54	0.04
wood ash	6.98	0.30
domestic ash	3.87	0.20
coal ash	8.86	0.38

Ice nucleation by combustion ash particles at conditions relevant to mixed-phase clouds

N. S. Umo et al.

Title Page

Abstract

Introduction

Conclusions

References

Tables

Figures

◀

▶

◀

▶

Back

Close

Full Screen / Esc

Printer-friendly Version

Interactive Discussion

Table 3. n_s parameterizations for combustion ash samples investigated in this report. The temperature ($^{\circ}\text{C}$) ranges for which the fits are valid are shown for each of the ash type.

Combustion ash type	$n_s(T)$ fit (cm^{-2})	R^2	Valid temperature range ($^{\circ}\text{C}$)
Coal fly ash (CFA)	$\exp[11.3014 - 1712.27 \cdot \exp(0.3153T)]$	0.9390	–15 to –31.5
Wood bottom ash	$\exp[-0.7818T - 11.884]$	0.9469	–11 to –36
Domestic bottom ash	$\exp[-15.5721 - 1.0386T - 0.0063T^2]$	0.9525	–12 to –35
Coal bottom ash	$\exp[-0.7305T - 13.802]$	0.9551	–13 to –36

Ice nucleation by combustion ash particles at conditions relevant to mixed-phase clouds

N. S. Umo et al.

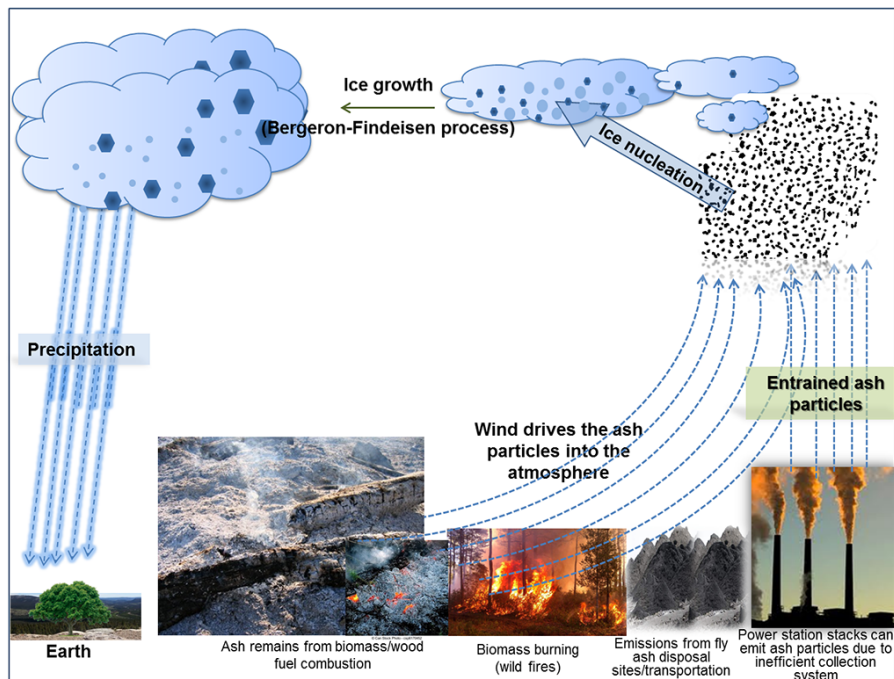


Figure 1. This schematic highlights the possible sources, emission routes and interactions of combustion ash particles in the troposphere. Combustion ash particles also participate in heterogeneous chemistry processes in the atmosphere. This study focuses on their ice nucleation activity at conditions relevant to mixed-phase clouds.

Title Page

Abstract

Introduction

Conclusions

References

Tables

Figures

◀

▶

◀

▶

Back

Close

Full Screen / Esc

Printer-friendly Version

Interactive Discussion

Ice nucleation by combustion ash particles at conditions relevant to mixed-phase clouds

N. S. Umo et al.

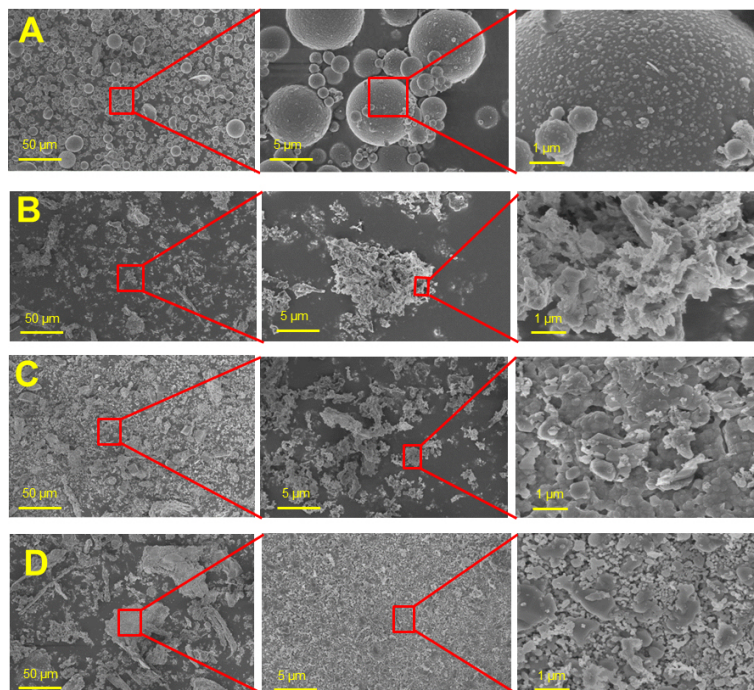


Figure 2. Scanning electron microscopy (SEM) images of CFA **(a)**, wood bottom ash **(b)**, domestic bottom ash **(c)**, and coal bottom ash **(d)** that were used for this ice nucleation study. All ash particles were sieved to $\leq 40 \mu\text{m}$ before the SEM images were taken. From left to right, the red boxes and their handles show different magnifications as presented with the scales on each SEM image panel.

Title Page

Abstract

Introduction

Conclusions

References

Tables

Figures

◀

▶

◀

▶

Back

Close

Full Screen / Esc

Printer-friendly Version

Interactive Discussion

Ice nucleation by combustion ash particles at conditions relevant to mixed-phase clouds

N. S. Umo et al.

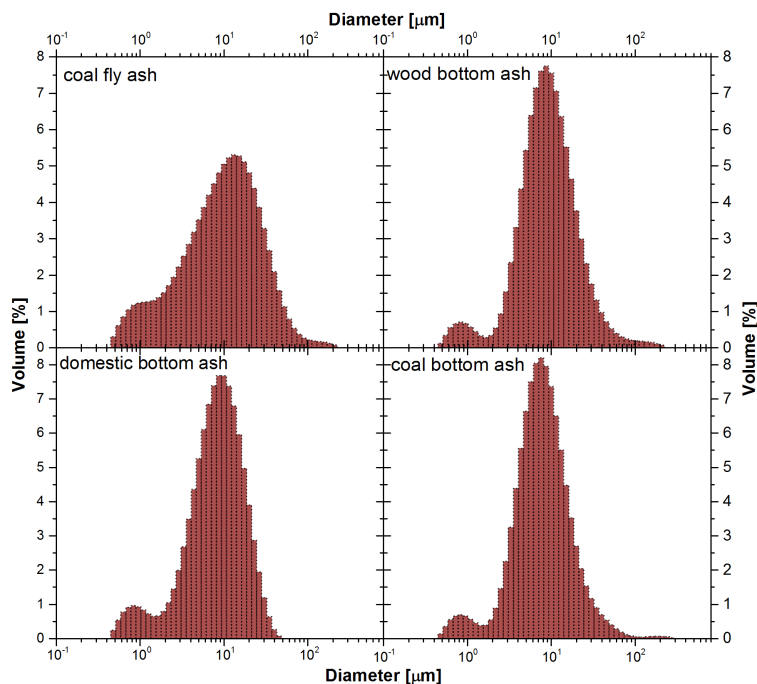


Figure 3. Particle size distribution of suspended combustion ash particles – coal fly ash (CFA), wood, domestic, and coal bottom ashes. The size distribution were measured after the ash suspensions were pulsated in an ultra-sonic bath for about 10 min and stirred for ~ 24 h before the laser diffraction measurement. Each plot of the size distribution shown for each ash sample is an average of three repeated measurements ($\sigma < 0.01$).

[Title Page](#)[Abstract](#)[Introduction](#)[Conclusions](#)[References](#)[Tables](#)[Figures](#)[◀](#)[▶](#)[◀](#)[▶](#)[Back](#)[Close](#)[Full Screen / Esc](#)[Printer-friendly Version](#)[Interactive Discussion](#)

Ice nucleation by combustion ash particles at conditions relevant to mixed-phase clouds

N. S. Umo et al.

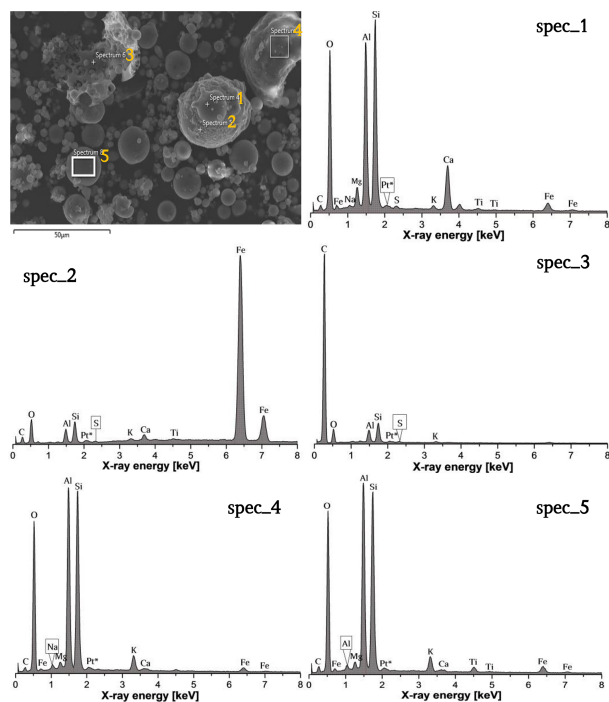


Figure 4. Elemental composition of CFA measured by energy dispersive X-ray spectroscopy (EDX) that was coupled to a scanning electron microscope (SEM). Platinum/Palladium (Pt/Pd) mixture was used to coat the samples before SEM/EDX spectra were taken; hence, it is asterisked on the spectra. These spectra were background corrected before making this plot. The ordinate (which is not shown) is intensity, in counts per second per energy unit (cps eV^{-1}). The spectra labels (spec_1, spec_2, . . . , spec_n) on the SEM images are the locations from which the EDX scanned.

Ice nucleation by combustion ash particles at conditions relevant to mixed-phase clouds

N. S. Umo et al.

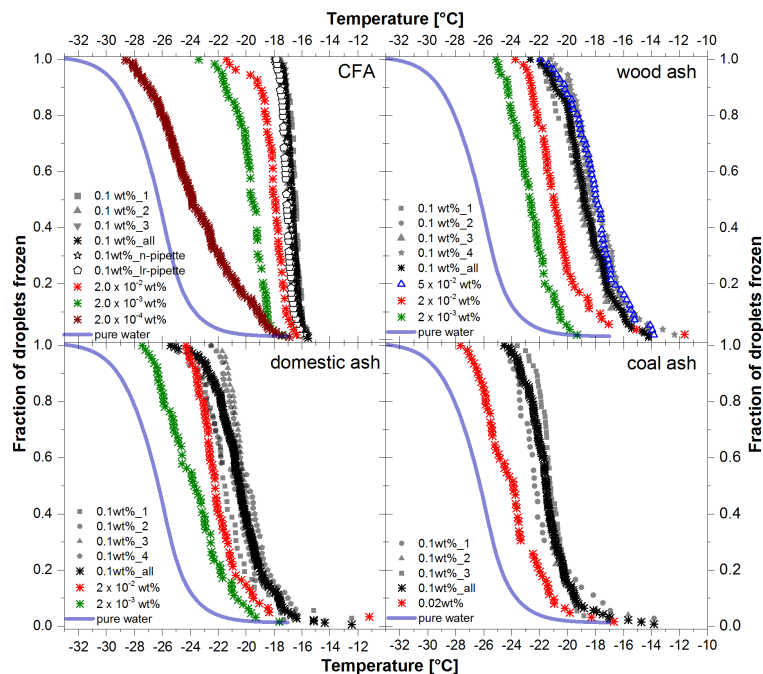


Figure 5. Fraction of droplets frozen (f_{ice}) from freezing experiments in the μ L-NIPI. Each panel shows freezing curves of droplets containing known concentrations (wt%) of CFA, wood, domestic, and coal bottom ashes. In all the panels, a fit to the background freezing (blue line) of ultra-pure water (18.2 M Ω cm resistivity) is plotted. All plots labelled as *0.1 wt%_all* on every panel are cumulative fractions frozen obtained from many repeat experiments. n-pipette represents normal pipette and lr-pipette is for low retention pipette. All experiments shown in this figure were performed with the n-pipette except indicated. The temperature uncertainty for μ L-NIPI is quoted as ± 0.4 K for all measurements and it is not plotted with the data points for the purpose of clarity.

Title Page

Abstract Introduction

Conclusions References

Tables Figures

◀ ▶

◀ ▶

Back Close

Full Screen / Esc

Printer-friendly Version

Interactive Discussion

Ice nucleation by combustion ash particles at conditions relevant to mixed-phase clouds

N. S. Umo et al.

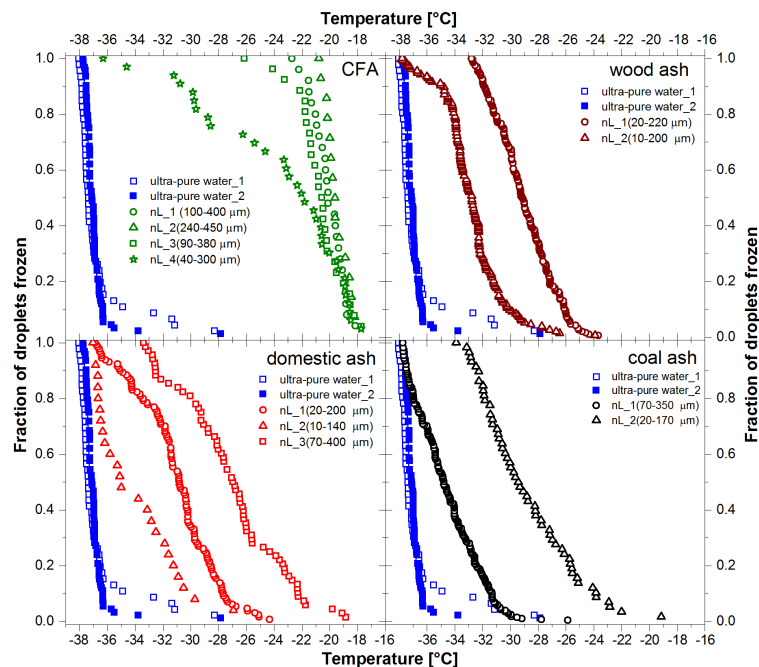


Figure 6. Fraction of droplets frozen (f_{ice}) from freezing experiment in the nL-NIPI. Each panel shows freezing curves of droplets containing 0.1 wt% of CFA, wood, domestic, or coal bottom ashes. The size range of the droplets varied from ~ 20 to $450 \mu\text{m}$ diameter. We give the range of the droplet diameter, but note that this is a rough guide to the size distribution since the distributions were commonly not log-normal. Most of the experiments in this figure were for droplets in the nanolitre (nL) volume range, but one run for the domestic ash was for picolitre droplets only (pL). For all panels, the royal blue squares (filled and unfilled) represent the freezing curve of ultra-pure water ($18.2 \text{ M}\Omega\text{cm}$ resistivity) on the same instrumental set-up with droplets ranging from $30\text{--}400 \mu\text{m}$ diameter for both runs. Uncertainty in the temperature measurements is quoted as $\pm 0.2 \text{ K}$.

Title Page

Abstract

Introduction

Conclusions

References

Tables

Figures

◀

▶

◀

▶

Back

Close

Full Screen / Esc

Printer-friendly Version

Interactive Discussion

Ice nucleation by combustion ash particles at conditions relevant to mixed-phase clouds

N. S. Umo et al.

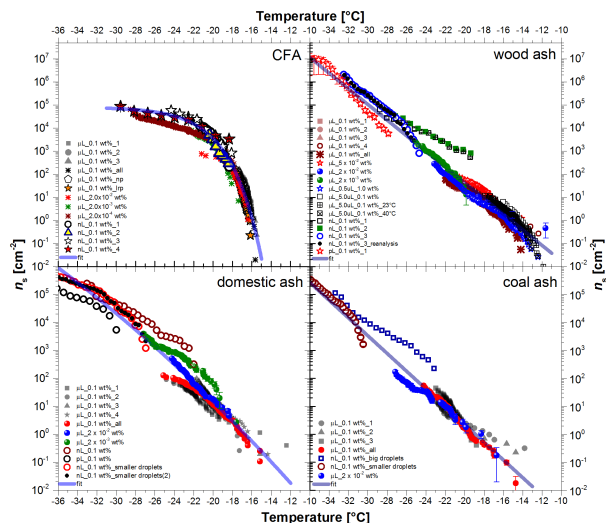


Figure 7. Ice nucleation active sites (n_s) distribution for CFA, wood bottom ash, domestic bottom ash, and coal bottom ash particles, obtained from freezing experiments in μL - and nL-NIPI. Each panel represents the cumulative number of nucleation active sites (n_s) on the ash particles calculated from the ice nucleation singular model and it covers all the temperature range explored during the freezing experiments. For the μL -NIPI experiments, n-pipette represents normal pipette and Ir-pipette is for low retention pipette – all experiments shown in this figure were performed with the n-pipette ($1.00 \pm 0.025 \mu\text{L}$) except indicated. On the wood bottom ash panel, the experiments indicated 23°C and 40°C were performed to test the effect of the initial temperature of the suspensions on its freezing ability. The equations for the n_s parameterizations and their valid temperatures for each of the combustion ashes are shown in Table 3. Estimated error bars are only shown for a selection of data sets for clarity and in many of these cases the error bars are smaller than the size of the data points.

Title Page

Abstract

Introduction

Conclusions

References

Tables

Figures

◀

▶

◀

▶

Back

Close

Full Screen / Esc

Printer-friendly Version

Interactive Discussion

Ice nucleation by combustion ash particles at conditions relevant to mixed-phase clouds

N. S. Umo et al.

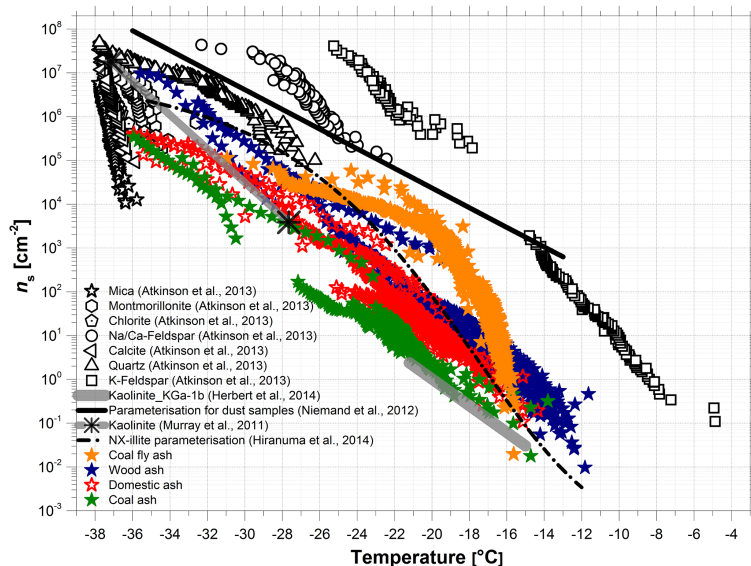


Figure 8. Comparison of ice nucleation active sites (n_s) distribution for combustion ashes and other mineral INPs such as mica, montmorillonite, chlorite, feldspar (Na/Ca) (albite), calcite, quartz, K-feldspar (microcline) taken from Atkinson et al. (2013), kaolinite (KGa-1b) from Herbert et al. (2014), and kaolinite from Murray et al. (2011). The solid and dotted black lines are parameterizations for the immersion freezing of desert dusts (Niemand et al., 2012) and NX-illite (Hiranuma et al., 2014), respectively. All coloured data points are for the different combustion ashes investigated in this present study.

Title Page

Abstract

Introduction

Conclusions

References

Tables

Figures

◀

▶

◀

▶

Back

Close

Full Screen / Esc

Printer-friendly Version

Interactive Discussion